An ion-implanted InP receiver for polarization resolved terahertz spectroscopy

E. Castro-Camus,[1] J. Lloyd-Hughes,[1] L. Fu,[2] H.H. Tan,[2] C. Jagadish,[2] and M. B. Johnston[1*]

[1]*Clarendon Laboratory, Department of Physics, University of Oxford, Parks Road, OX1 3PU, Oxford United Kingdom.*

[2]*Department of Electronic Materials Engineering, Research School of Physical Sciences and Engineering, Institute of Advanced Studies, Australian National University, Canberra ACT 0200, Australia.*

[*]*Corresponding author: m.johnston@physics.ox.ac.uk*

Abstract: We report on the construction, optical alignment and performance of a receiver which is capable of recording the full polarization state of coherent terahertz radiation. The photoconductive detector was fabricated on InP which had been implanted with Fe^+ ions. The device operated successfully when it was gated with near infrared femtosecond pulses from either a Ti:sapphire laser oscillator or a 1 kHz regenerative laser amplifier. When illuminated with terahertz radiation from a typical photoconductive source, the optimized device had a signal to noise figure of 100:1 with a usable spectral bandwidth of up to 4 THz. The device was shown to be very sensitive to terahertz polarization, being able to resolve changes in polarization of 0.34 degrees. Additionally, we have demonstrated the usefulness of this device for (i) polarization sensitive terahertz spectroscopy, by measuring the birefringence of quartz and (ii) terahertz emission experiments, by measuring the polarization dependence of radiation generated by optical rectification in (110)-ZnTe.

OCIS codes: (230.5440) Polarization-sensitive devices; (300.6270) Spectroscopy, far infrared; (320.7080) Ultrafast devices.

References and links

1. C. A. Schmuttenmaer, "Exploring dynamics in the far-infrared with terahertz spectroscopy," Chem. Rev. **104,** 1759–1779 (2004).
2. R. Huber, F. Tauser, A. Brodschelm, M. Bichler, G. Abstreiter, and A. Leitenstorfer, "How many-particle interactions develop after ultrafast excitation of an electron-hole plasma," Nature **414,** 286–289 (2001).
3. J. Lloyd-Hughes, T. Richards, H. Sirringhaus, E. Castro-Camus, L. M. Herz, and M. B. Johnston, "Charge trapping in polymer transistors probed by terahertz spectroscopy and scanning probe potentiometry," Appl. Phys. Lett. **89,** 112101 (2006).
4. F. Gao, J. F. Whitaker, Y. Liu, C. Uher, C. E. Platt, and M. V. Klein, "Terahertz transmission of a $Ba_{1-x}K_xBiO_3$ film probed by coherent time-domain spectroscopy," Phys. Rev. B **52,** 3607–3613 (1995).
5. M. B. Johnston, L. M. Herz, A. Khan, A. Köhler, A. G. Davies, and E. H. Linfield, "Low-energy vibrational modes in phenylene oligomers studied by THz time domain spectroscopy," Chem. Phys. Lett. **377,** 256–262 (2003).
6. Y. Q. Chen, H. B. Liu, Y. Q. Deng, D. Schauki, M. J. Fitch, R. Osiander, C. Dodson, J. B. Spicer, M. Shur, and X. C. Zhang, "THz spectroscopic investigation of 2,4-dinitrotoluene," Chem. Phys. Lett. **400,** 357–361 (2004).

#81506 - $15.00 USD Received 12 Apr 2007; revised 7 May 2007; accepted 21 May 2007; published 24 May 2007

7. S. Kono, M. Tani, and K. Sakai, "Ultrabroadband photoconductive detection: Comparison with free-space electro-optic sampling," Appl. Phys. Lett. **79,** 898–900 (2001).
8. D. H. Auston and M. C. Nuss, "Electrooptic generation and detection of femtosecond electrical transients," IEEE J. Quantum Electron. **24,** 184–197 (1988).
9. P. R. Smith, D. H. Auston, and M. C. Nuss, "Subpicosecond photoconducting dipole antennas," IEEE J. Quantum Electron. **24,** 255–260 (1988).
10. Y. C. Shen, P. C. Upadhya, H. E. Beere, E. H. Linfield, A. G. Davies, I. S. Gregory, C. Baker, W. R. Tribe, and M. J. Evans, "Generation and detection of ultrabroadband terahertz radiation using photoconductive emitters and receivers," Appl. Phys. Lett. **85,** 164–166 (2004).
11. M. Suzuki and M. Tonouchi, "Fe-implanted InGaAs photoconductive terahertz detectors triggered by 1.56μm femtosecond optical pulses," Appl. Phys. Lett. **86,** 163504 (2005).
12. M. Tani, K. Sakai, and H. Mimura, "Ultrafast photoconductive detectors based on semi-insulating GaAs and InP," Jpn. J. Appl. Phys. Part 2 **36,** L1175–L1178 (1997).
13. J. Lloyd-Hughes, S. K. E. Merchant, L. Fu, H. H. Tan, C. Jagadish, E. Castro-Camus, and M. B. Johnston, "Influence of surface passivation on ultrafast carrier dynamics and terahertz radiation generation in GaAs," Appl. Phys. Lett. **89,** 232102 (2006).
14. E. Castro-Camus, J. Lloyd-Hughes, and M. B. Johnston, "Three-dimensional carrier-dynamics simulation of terahertz emission from photoconductive switches," Phys. Rev. B **71,** 195301 (2005).
15. J. Lloyd-Hughes, E. Castro-Camus, and M. B. Johnston, "Simulation and optimisation of terahertz emission from InGaAs and InP photoconductive switches," Solid State Commun. **136,** 595–600 (2005).
16. A. Hussain and S. R. Andrews, "Dynamic range of ultrabroadband terahertz detection using GaAs photoconductors," Appl. Phys. Lett. **88,** 143514 (2006).
17. J. F. O'Hara, J. M. O. Zide, A. C. Gossard, A. J. Taylor, and R. D. Averitt, "Enhanced terahertz detection via ErAs:GaAs nanoisland superlattices," Appl. Phys. Lett. **88,** 251119 (2006).
18. E. Castro-Camus, J. Lloyd-Hughes, M. B. Johnston, M. D. Fraser, H. H. Tan, and C. Jagadish, "Polarization-sensitive terahertz detection by multicontact photoconductive receivers," Appl. Phys. Lett. **86,** 254102 (2005).
19. F. G. Sun, G. A. Wagoner, and X. C. Zhang, "Measurement of free-space terahertz pulses via long-lifetime photoconductors," Appl. Phys. Lett. **67,** 1656–1658 (1995).
20. T. A. Liu, M. Tani, M. Nakajima, M. Hangyo, K. Sakai, S. Nakashima, and C. L. Pan, "Ultrabroadband terahertz field detection by proton-bombarded InP photoconductive antennas," Opt. Express **12,** 2954–2959 (2004).
21. T. A. Liu, M. Tani, M. Nakajima, M. Hangyo, and C. L. Pan, "Ultrabroadband terahertz field detection by photoconductive antennas based on multi-energy arsenic-ion-implanted GaAs and semi-insulating GaAs," Appl. Phys. Lett. **83,** 1322–1324 (2003).
22. J. B. Johnson, "Thermal Agitation of Electricity in Conductors," Phys. Rev. **32,** 97 (1928).
23. H. Nyquist, "Thermal Agitation of Electric Charge in Conductors," Phys. Rev. **32,** 110–113 (1928).
24. R. Sarpeshkar, T. Delbruck, and C. A. Mead, "White-noise in mos-transistors and resistors," IEEE Circuit Devices Mag. **9,** 23–29 (1993).
25. F. N. Hooge, "1/f noise sources," IEEE Trans. Electron Devices **41,** 1926–1935 (1994).
26. D. Grischkowsky, S. Keiding, M. van Exter, and C. Fattinger, "Far-infrared time-domain spectroscopy with terahertz beams of dielectrics and semiconductors," J. Opt. Soc. Am. B **7,** 2006–2015 (1990).
27. E. Castro-Camus, D.Phil thesis, University of Oxford, 2006.
28. G. Giraud, J. Karolin, and K. Wynne, "Low-frequency modes of peptides and globular proteins in solution observed by ultrafast OHD-RIKES Spectroscopy," Biophys. J. **85,** 1903–1913 (2003).
29. A. Markelz, S. Whitmire, J. Hillebrecht, and R. Birge, "THz time domain spectroscopy of biomolecular conformational modes," Phys. Med. Biol. **47,** 3797–3805 (2002).
30. J. Xu, K. W. Plaxco, and S. J. Allen, "Probing the collective vibrational dynamics of a protein in liquid water by terahertz absorption spectroscopy," Protein Sci. **15,** 1175–1181 (2006).

1. Introduction

Until two decades ago the far-infrared or terahertz (THz) band of the spectrum ($\sim$100 GHz - 10 THz) remained relatively unreachable to spectroscopists owing to the lack of appropriate sources and detectors of THz radiation. The development of terahertz time-domain spectroscopy[1] (THz-TDS) has accelerated fundamental and applied research in this important spectral region[2, 3, 4, 5, 6]. The THz-TDS technique is based on the generation of single cycles of radiation with sub-picosecond duration, and the detection of the electric field of these transients[7].

Electro-optic sampling[8] and photoconductive detection[9] are the primary methods of measuring the electric field of such single-cycle THz transients. A photoconductive receiver

#81506 - $15.00 USD Received 12 Apr 2007; revised 7 May 2007; accepted 21 May 2007; published 24 May 2007

consists of a pair of metallic contacts deposited on a semiconducting material, typically low-temperature-grown GaAs [10] or an ion-implanted semiconductor [11, 9]. The performance of photoconductive switches is closely linked to the properties of the semiconductors from which they are fabricated[12, 13]. Recently there has been considerable interest in developing semiconducting materials which exhibit optimal charge carrier dynamics for THz device applications[14, 15, 16, 17].

Established methods of detecting THz transients, including electro-optic sampling and conventional photoconductive detection, have the disadvantage of detecting only one component of the THz electric field at a time. Thus the signal measured is always a projection of the full polarization state onto one polarization component. In effect this complicates the use of THz-TDS when studying birefringent or optically active materials. For example in a standard spectroscopic measurement of a birefringent material, unless one is careful, a rotation of the polarization may be incorrectly interpreted as an absorption feature. Recently a novel three-contact photoconductive detector capable of detecting the full polarization state of a THz pulse was reported[18].

In this paper a characterization of the signal-to-noise, spectral response and polarization resolution of a three contact photoconductive detector based on Fe^+-ion implanted InP is presented. The main noise sources are identified and the optimal operation conditions are reported. To illustrate the performance of the device in spectroscopic measurements the results from two sets of experiments utilizing the polarization sensitive detector are presented.

2. Polarization sensitive THz receiver

Our polarization sensitive detector was designed to detect simultaneously two orthogonal components of the electric field from a THz transient. A description of the design and fabrication of the device has been given previously[18], and a summary of the principles of photoconductive detector operation can be found in Refs. [19, 12]. Briefly, the device consisted of three gold electrodes evaporated onto a semiconductor (Fe^+ ion-implanted InP) substrate such that there were two orthogonal photoconductive gap regions between the electrodes (as shown in Fig. 1(a)). The two electrodes that were at right angles to each other were connected to two separate lock-in amplifiers, while the third contact was earthed. To operate such a detector a THz pulse and a collinear femtosecond laser "gate" pulse are focused onto the central region of the device so that both gap regions are illuminated by both radiation pulses. The "gate" creates free charge carriers in the region of the semiconductor between the electrodes, thereby allowing current to flow under the influence of the electric field applied by the THz pulse. As the typical lifetime of charge carriers is greater than the duration of the THz pulse, one may assume that the current recorded between the electrodes and earth is proportional to the integral of the electric field from the THz pulse that arrives after the gate pulse.[19, 12] By using an optical time-delay line to vary the arrival time of subsequent laser "gate" pulses with respect to the THz pulses, and then differentiating the time-delay dependent signals from the two lock-in amplifiers, a polarization resolved measurement of the THz transient is achieved.

In order to characterize the performance of the three-contact photoconductive sensor and determine the optimal conditions of use the following experimental configuration was used. The photoconductive receiver was mounted in the terahertz time domain spectrometer shown schematically in Fig. 1. A 400 μm gap semi-insulating-GaAs photoconductive emitter was excited with 10 fs pulses at an average power of 360 mW provided by a Ti:sapphire oscillator with repetition rate of 75 MHz and center wavelength of 790 nm. The photoconductive emitter was mounted on a rotation stage in order to control the terahertz polarization angle θ. The emitter was biased with a square wave of $\pm$120 V amplitude, and frequency controllable from dc to 50 kHz. A dielectric beam splitter was used to split off 40 mW of the original laser beam, which

#81506 - $15.00 USD Received 12 Apr 2007; revised 7 May 2007; accepted 21 May 2007; published 24 May 2007

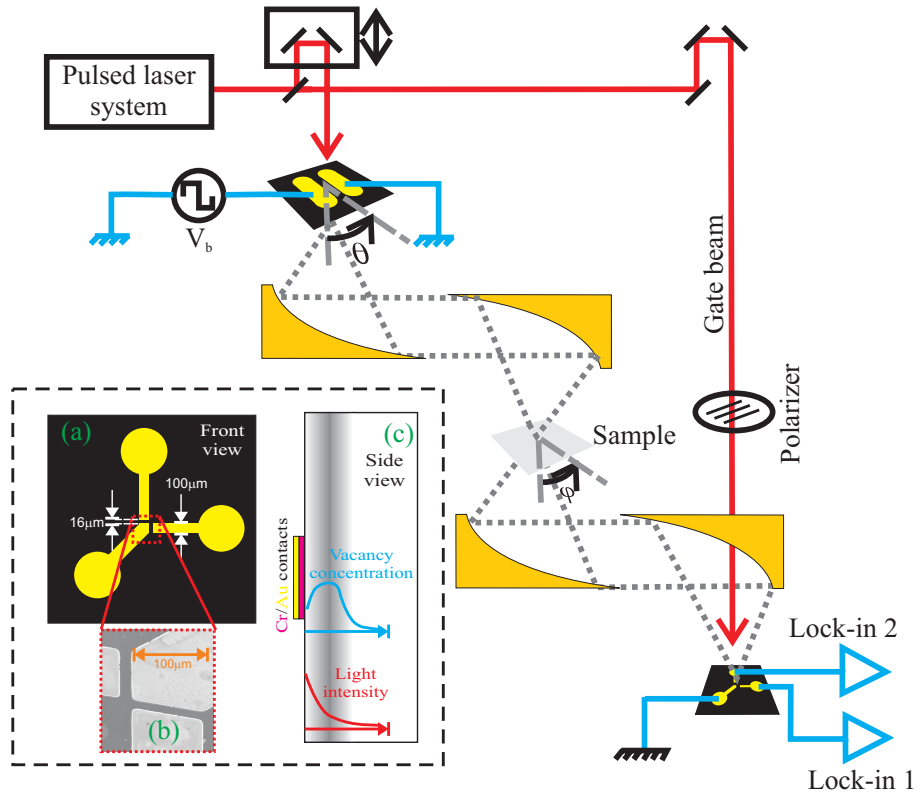

Fig. 1. Schematic diagram of a terahertz time domain spectrometer. A part of the laser pulse was used to excite a biased photoconductive switch. The switch was mounted on a rotation stage to allow the angle of polarization to be adjusted. The remainder of the laser pulse formed the "gate beam", which passed through a hole that had been drilled in an off-axis parabolic mirror, used to focus THz radiation onto the polarization sensitive THz detector. Inset: (a) Contact geometry of the polarization sensitive THz receiver, including (b) an electron micrograph of the gap region. (c) A schematic diagram of a cross section through the device, illustrating that the region of vacancies generated by ion implantation overlaps with the region of photo-excited carriers.

was used to gate the photoconductive receiver. The intensity of the gate beam was controlled by rotating a polarizer. The current between the terminals of the photoconductive switch was recorded using two separate lock-in amplifiers with their time constants set to 100 ms. Both amplifiers were phase-locked to the frequency of the bias voltage signal that was applied to the THz emitter. One lock-in amplifier was used to measure a signal related to the horizontal component of the terahertz electric field while the second simultaneously measured the vertical component.

Appropriate alignment of the three contact structure is necessary in order to obtain good performance as a polarization sensitive receiver. In order to align the detector the following procedure was used. Firstly, the gate beam was blocked and the terahertz emitter replaced with a diffuser (such as a piece of bond or tracing paper) in order to produce a point source of 800 nm radiation at the emitter position (see Fig. 1). The scattered laser radiation from the diffuser is collected by the off-axis parabolic mirrors, and thus follows the THz radiation path and focused

#81506 - $15.00 USD Received 12 Apr 2007; revised 7 May 2007; accepted 21 May 2007; published 24 May 2007

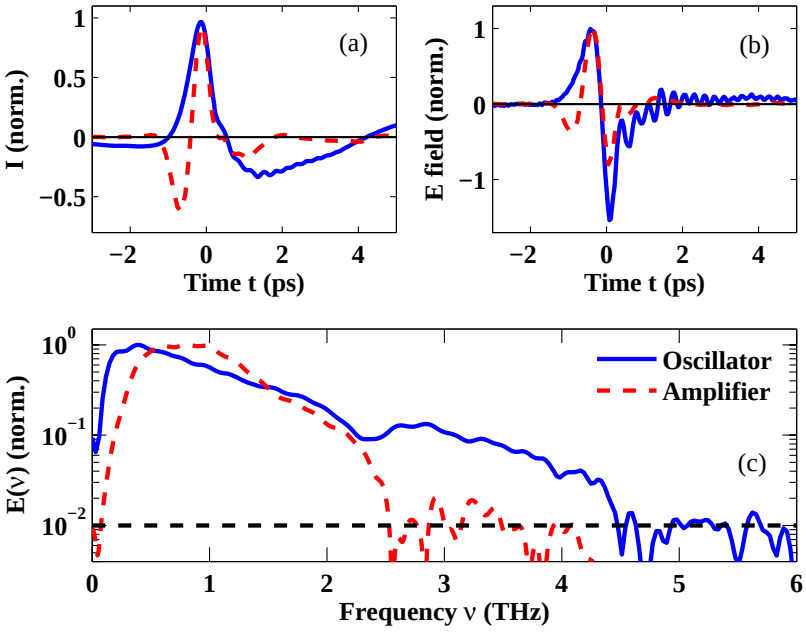

Fig. 2. (a) Current recorded through the "horizontal" contact of a 3-contact polarization sensitive receiver in a THz-TDS spectrometer driven by a laser oscillator (solid blue line) and a laser amplifier (dashed red line) as a function of gate delay time. (b) Time-domain electric field (horizontal component) of a THz transient produced in the oscillator (solid blue line) and amplifier (dashed red line) based THz-TDS systems. These data are obtained by differentiating the data shown in (a) with respect to delay time. (c) The amplitude spectrum of the electric field transients presented in (b). The dotted line indicates the noise floor for these measurements.

onto the three contact receiver. Secondly, the three degrees of freedom in the detector's position were adjusted to minimize the resistance between two of the contacts of the device. Thirdly, the terahertz generation beam was blocked and the gate beam unblocked. Then the gate beam was adjusted to minimize the resistance between the same two contacts, again leaving the position of the receiver unchanged. Finally the position of the receiver was adjusted to balance and minimize the resistance of both gaps of the structure. By following this method the device could quickly and reproducibly be implemented in a range of laser oscillator and amplifier driven THz-TDS systems.

A typical set of data obtained from the detector is shown in Fig. 2. For clarity only the horizontal component of the THz electric field is displayed in the figure. Figure 2(a) shows the current recorded as a function of time-delay between the THz pulse and the femtosecond gate pulse. In order to convert these data into the electric field transient shown in Fig. 2(b) the data were differentiated with respect to time. The amplitude spectrum was then obtained by Fourier transforming those data as shown in Fig. 2(c).

An important characteristic of any broadband THz receiver is its bandwidth. The full spectral width of the detector in the THz-TDS system described above is a respectable $\sim$3 THz at -10 dB. Note that the spectrum covers the range from $\sim$50 GHz to approximately 4 THz before the signal reaches the noise floor. The polarization resolved detector was also tested in a THz-

#81506 - $15.00 USD Received 12 Apr 2007; revised 7 May 2007; accepted 21 May 2007; published 24 May 2007

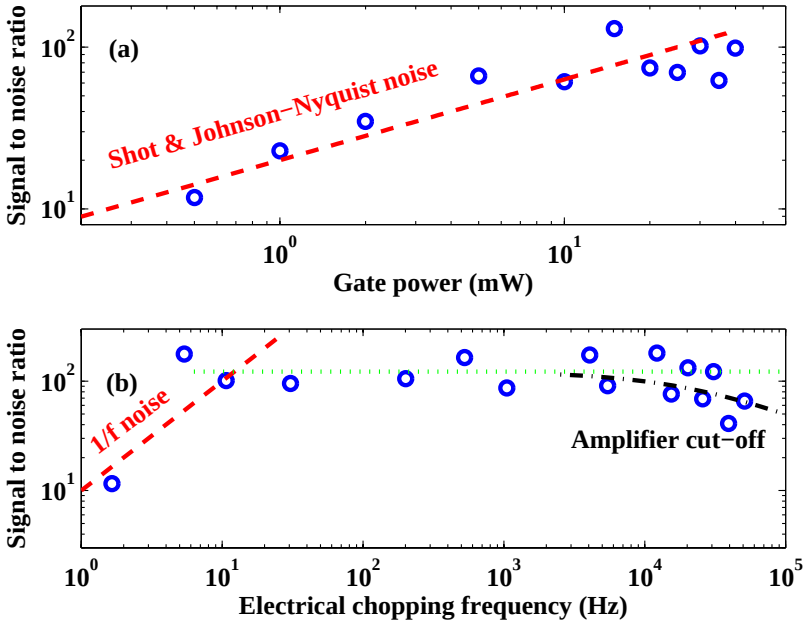

Fig. 3. Signal to noise ratio measured for the three-contact photoconductive receiver as a function of gate power. The (blue) circles are the measured values, the dashed (red) line is a $P_G^{1/2}$ line related to the Shot and Johnson-Nyquist noise. (b) Signal to noise ratio measured for the three-contact photoconductive receiver as a function of emitter chopping frequency. The (blue) circles are the measured values, the dashed (red) a linear function of frequency related to the $1/f$-noise. The dotted (green) line is an indication of the SNR level independent of the frequency. An additional dash-dotted line indicates the low-pass filter behavior of the high voltage amplifier driving the photoconductive emitter.

TDS system driven by a regenerative amplifier (1 kHz repetition rate, 1 mJ pulse energy, 40 fs pulse duration). In this experiment the photoconductive THz source was replaced with an optical rectification source (2mm-thick (110)-ZnTe). The bandwidth of the amplifier system was less than that of the oscillator driven system, mainly as a result of differences in the spectral content of the two THz sources. However, the two systems showed a similar signal to noise performance in the 0.5-2.2 THz band, illustrating the flexibility of the polarization sensitive receiver.

3. Noise performance

In contrast to most optical measurements, where signal refers to irradiance, here the electric field is the variable to be measured. Therefore it is important to define what it is understood by *signal* and *noise*. In this paper *signal* refers to the peak-to-peak current over one time-domain scan, and the standard deviation of the difference of two consecutive scans with identical parameters will be referred to as the *noise*.

The two main sources of noise affecting measurements made with a photoconductive receiver are Johnson-Nyquist and laser shot noise[20, 21, 12]. Johnson-Nyquist noise is caused by thermal fluctuations of the charge carriers in a material [22, 23, 24]. The root-mean-square

#81506 - $15.00 USD Received 12 Apr 2007; revised 7 May 2007; accepted 21 May 2007; published 24 May 2007

Johnson-Nyquist noise current is

$$I_{\mathrm{J-N}} = \sqrt{\frac{4k_B T \Delta f}{R}} \tag{1}$$

where k_B is Boltzman's constant, T is the temperature, Δf is the measurement bandwidth (usually limited by the lock-in amplifier's phase sensitive detector $\sim$0.01 Hz) and R is the resistance of the receiver, which is inversely proportional to the gating power, and therefore $I_{\mathrm{J-N}} \propto P_G^{1/2}$. The case of laser shot noise shows a gate-power dependence of the form $I_{\mathrm{Shot}} \propto P_G^{1/2}$.[20] Given that the carrier density in the detector is proportional to P_G, the signal amplitude $I \propto P_G$,[12] and therefore the signal to noise ratio is expected to show a behavior $SNR \propto P_G^{1/2}$ in the regime where the laser shot and Johnson-Nyquist noises dominate.

In order to characterize the noise performance of the three-contact THz receiver pairs of scans were taken with the gate power varied from 0 to 40 mW. In Fig. 3 the measured signal to noise ratio at various gating powers is shown. In the figure the dashed curve indicates the $P_G^{1/2}$ dependence associated with shot and Johnson-Nyquist noise.

Both Johnson-Nyquist and shot noise are considered to be "white" noise, namely they are independent of frequency. In semiconductor devices a relatively large contribution to the noise is often associated with $1/f$-noise. This is related to fluctuations in the conductivity when the device is operated at low enough frequencies($<$ 10kHz).[25] In order to quantify how relevant this $1/f$-noise contribution is in the polarization sensitive photoconductive receiver, a series of measurements were taken by setting the gating power to 40 mW and varying the electrical chopping frequency of the photoconductive emitter. The signal to noise ratio for these measurements is presented in Fig. 3. A dashed curve on the figure is a $SNR \propto f$ line fitting just the first three experimental points. This plot shows that for chopping frequencies above 10 Hz the noise present in the measurements is white, and therefore is primarily the result of shot and Johnson-Nyquist noise. The drop in the signal to noise ratio for frequencies over $\sim$20 kHz is not associated to a variation of the noise level, but owing to a drop in the signal amplitude caused by the frequency response of the amplifier driving the photoconductive emitter. This feature was modeled as a simple first order low pass filter (shown as a dash-dotted line).

4. Polarization sensitivity

One of the most important characteristics to assess a three-contact photoconductive receiver is its effectiveness as a polarization sensitive detector. Linearly polarized THz pulses were produced at various polarization angles by rotating the photoconductive emitter in the terahertz time-domain system already described. A three-dimensional projection plot of terahertz pulses measured with the polarization sensitive detector and emitted at 0, 45 and 90 $^\circ$ is presented in Fig. 4. This three-dimensional projection plot shows qualitatively that the 3-contact receiver acts as a polarization sensitive detector, however it is desirable to have a quantitative characterization of how sensitive the detector is to changes of polarization.

The photoconductive emitter was mounted in a high precision (better than 0.06 $^\circ$) motorized rotation stage and the THz electric field was recorded as function of time and angle. Thus the (linear) polarization of the emitted THz pulse was varied in 0.1 $^\circ$ steps from 0 to 1 $^\circ$ and using larger steps up to 5°. The polarization angle was calculated as θ_{meas}=arctan$[E_V(t=0)/E_H(t=0)]$, where $E_V(t=0)$ and $E_H(t=0)$ are the peak values of the horizontal and vertical components of the electric field in the time domain. The measured values are shown on the inset of Fig. 4. The standard deviation of the measured values from the $\theta_{\mathrm{meas}} = \theta$ line was determined to be $\sigma_\theta = 0.34^\circ$, which can be quoted as the angular resolution limit of the system. The angular resolution of the device may be even better than this resolution as it represents a limit of the

#81506 - $15.00 USD Received 12 Apr 2007; revised 7 May 2007; accepted 21 May 2007; published 24 May 2007

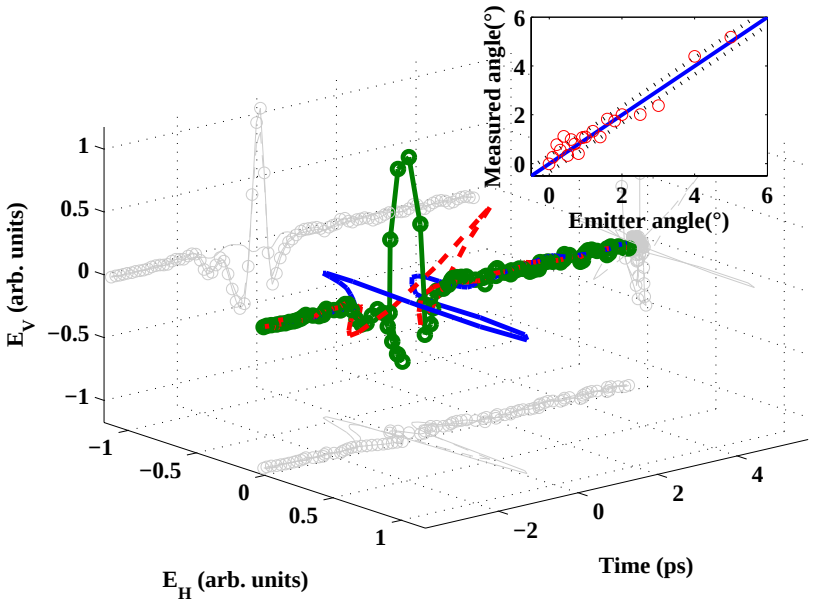

Fig. 4. Demonstration of the measurement capability of the three contact THz receiver. Three dimensional representation of electric fields measured as a function of time with the THz emitter (and hence THz polarization) rotated to 0°, 45° and 90°. Inset: Measured electric field polarization angle as a function of the emitter rotation angle (circles). The continuous line is $\theta_{\text{meas}} = \theta$, which is the expected behavior. The standard deviation of the measured points from the line was calculated to be 0.34° and is indicated with the dotted lines.

system as a whole to resolve polarization. Slight misalignment of the off-axis parabolic mirrors in the spectrometer may well be a more significant limit to the measurements than the device itself.

5. Polarization resolved THz transmission spectroscopy

The performance and versatility of the polarization sensitive THz detector is best illustrated by implementing the device in a standard THz-TDS transmission spectrometer. We chose to measure the properties of a quartz quarter wave plate. Quartz is known to be birefringent at THz frequencies [26], hence by choosing a certain thickness of X-cut quartz it is possible to fabricate a zeroth order wave-plate.

We placed a 1.55mm thick plate of X-cut quartz, which was designed to function as a quarter wave-plate at 1 THz, in the "sample" position of the spectrometer shown in Fig. 1. The wave-plate was positioned so that its ordinary and extraordinary axes pointed in the horizontal and vertical directions respectively. The THz emitter was orientated so that it emitted linearly polarized pulses with a plane of polarization at 45° to the horizontal.

The electric field of the THz transient once it had passed through the wave-plate is displayed in Fig. 5(a). In this figure the two electric field components are plotted against time, thereby showing that the electric field vector traces out a right-handed helix. We also performed another measurement after rotating the quartz wave-plate by 90° (thereby swapping the ordinary and extraordinary axes). Figure 5(b) shows the left-handed electromagnetic transient measured in this case.

#81506 - $15.00 USD Received 12 Apr 2007; revised 7 May 2007; accepted 21 May 2007; published 24 May 2007

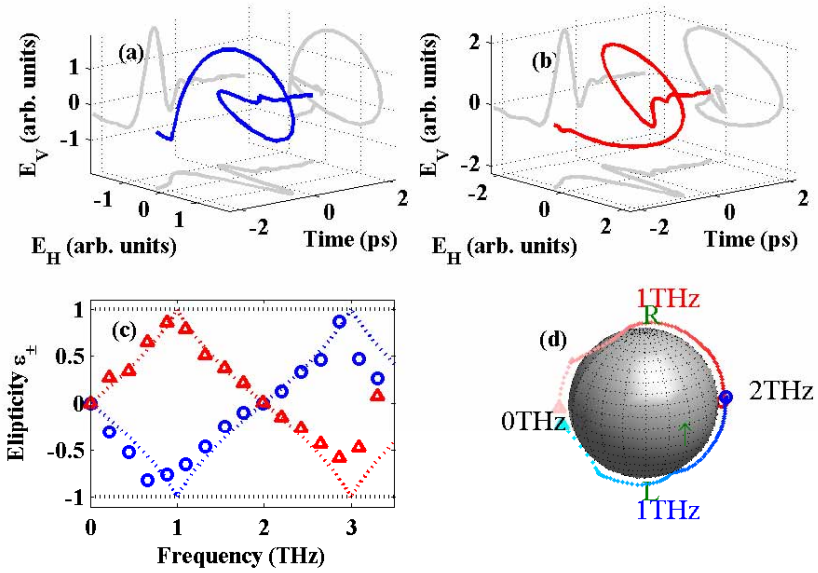

Fig. 5. (a) Three dimensional projection plot of a terahertz pulse after propagating through a retardation plate made of quartz (1.55 mm thick). The ordinary axis is aligned in the direction of the vertical component of the THz field E_V. The pulse has non-planar polarization. (b) An analogous plot inverting the ordinary and extraordinary axes of the quartz sample. (c) Shows the ellipticity extracted from the two pulses shown in (a) (circles) and (b) (triangles), the dotted lines are the calculated ellipticity. (d) Shows polarization states extracted from the two measured pulses in (a) (blue) and (b) (red) on the Poincaré sphere. The trajectories run from 0 (light color) to 2 THz (dark color) passing through the poles (circular polarization states) at around 1 THz (The points were plotted above instead of on the surface for clarity).

Apart from the "handedness" of the THz pulse it is difficult to extract more quantitative information from these time-domain data. However, from such data it is straightforward[27] to calculate the ellipticity of the transient as a function of frequency. A representation of the frequency dependent ellipticity of the measured THz transient is shown in Fig. 5(c) along with the calculated ellipticity (dashed lines). It can been seen that the quartz wave-plate works as a quarter wave-plate at 1 THz but as a half wave-plate at 2 THz. Therefore, after a linearly polarized THz transient has passed through such a wave-plate it is difficult to characterize it as "circularly", or "linearly" polarized since different frequency components of the pulse have significantly different states of polarization.

A useful way of representing the full polarization state of a broadband THz pulse is as a trajectory on the Poincaré sphere, as shown in Fig. 5(d). Note that each point on the trajectory corresponds to a different Fourier component of the THz transient.

As illustrated in this wave-plate example, a polarization resolved THz measurement may be used to characterize the properties of a wave-plate, or any birefringent material, in a single measurement. The full polarization state of a THz pulse can appear complicated, however it holds a wealth of information about the material through which the pulse has passed.

#81506 - $15.00 USD Received 12 Apr 2007; revised 7 May 2007; accepted 21 May 2007; published 24 May 2007

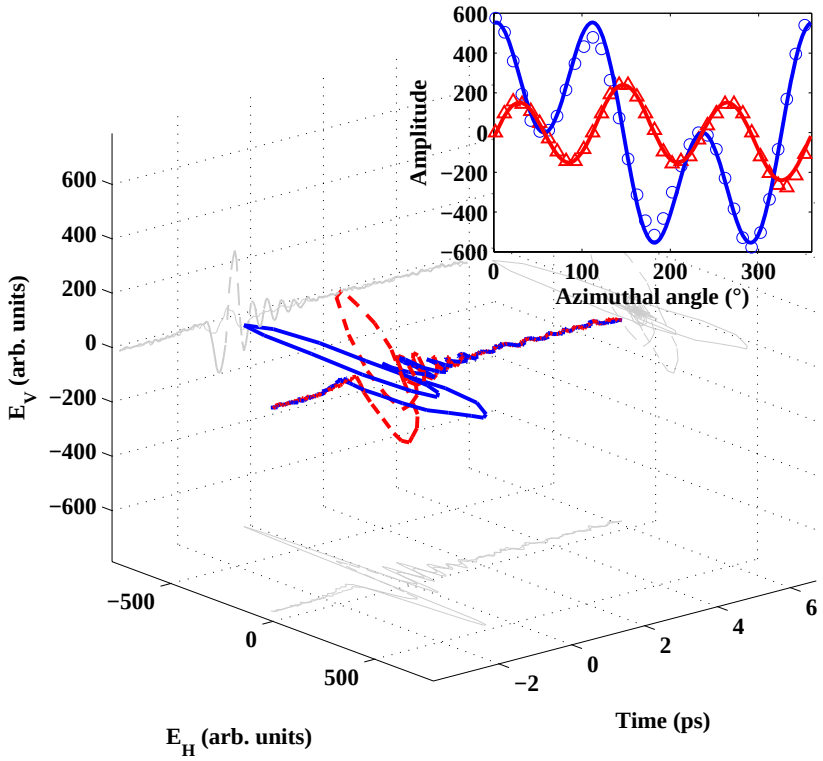

Fig. 6. A demonstration of polarization resolved THz emission spectroscopy. Projection plot of THz electric field emitted from (110)-ZnTe at 0° (solid blue line) and 30° (dashed red line). Inset: Peak THz electric field (horizontal: circles, vertical: triangles) components emitted by ZnTe as function of angle with respect to the pump polarization (horizontal).

6. Polarization resolved THz emission spectroscopy

Another interesting application of the detector is as a tool for THz emission spectroscopy. Optical rectification of femtosecond laser pulses in (110)-oriented ZnTe crystals is a popular method for generating coherent THz transients. The amplitude and polarization of the THz radiation produced are sensitive to the orientation of the ZnTe crystal with respect to the polarization of the laser pulse, since the mechanism depends on the second order electrical susceptibility tensor of the crystal. Optical rectification in ZnTe is well understood, however in practise determining the best azimuthal angle to orient a (110)-ZnTe crystal for high efficiency THz generation can be time consuming when using detectors that can only resolve one polarization component.

Terahertz transients were generated in a 1-mm thick (110)-ZnTe crystal illuminated with pulses from the laser amplifier described above. Figure 6 shows two sets of data recorded with the polarization sensitive receiver when the $\langle 1\bar{1}1 \rangle$ direction of the ZnTe crystal was rotated to an azimuthal angle of 0° and 30° with respect to the (horizontal) polarization of the laser pulse. By acquiring such traces and rotating the ZnTe crystal the optimum geometry for THz generation (and hence crystallographic orientation) is found quickly. The inset in Fig. 6 shows the peak vertical and horizontal components of terahertz transients generated from the ZnTe crystal as a function of azimuthal angle, recorded in 10 ° increments. These data closely match the theoretical relation shown by the solid lines.

#81506 - $15.00 USD Received 12 Apr 2007; revised 7 May 2007; accepted 21 May 2007; published 24 May 2007

The simultaneous measurement of two orthogonal components of the terahertz electric field is a powerful method of performing THz emission experiments, as the technique acquires all electric field data, thereby avoiding ambiguities present when recording data as a projection. Additionally this method provides a fast and convenient method of finding the crystallographic orientation of a THz emitter.

7. Conclusions

The performance of a polarization sensitive THz receiver was found to improve significantly with increasing gating power (up to 40 mW) owing to a sublinear increase in Johnson-Nyquist and laser shot noise. The signal to noise ratio was found to be almost constant as a function of frequency except for very low frequencies (<10 Hz) where $1/f$ noise dominates. These two measurements show that the receiver has a dynamic range of around two decades (40 dB) under optimal operation conditions, the usable bandwidth of the receiver was found to be $\sim$4 THz and the polarization angular resolution $\sim 0.34^\circ$. This integrated three-contact detector is the first step to extend terahertz time-domain spectroscopy to a polarization resolved technique, allowing the study of broadband polarization-dependent quantities such as birefringence, optical activity and circular dichroism in the terahertz band.

We have reported on two experiments which demonstrate that the detector is well suited to THz transmission and emission spectroscopy of anisotropic materials. There are many possible applications for this detector. Of particular interest to the biochemistry community is the study of vibrational modes of biomolecules like proteins and nucleic acids. The importance of polarization resolved terahertz studies of this type is currently promoting collaboration between the structural biology and the terahertz communities, to develop novel experimental techniques that allow such measurements[28, 29, 30]. The detector characterized in this work could be a key component in the construction of a terahertz vibrational circular dichroism spectrometer.

Acknowledgments

The authors would like to thank Gabriella Chapman and Oxford Materials for the scanning electron micrograph shown in Fig. 1. Financial support for this work was provided by the Royal Society, the Engineering and Physical Sciences Research Council (UK), and the Australian Research Council.

#81506 - $15.00 USD Received 12 Apr 2007; revised 7 May 2007; accepted 21 May 2007; published 24 May 2007